

Contents lists available at [ScienceDirect](https://www.sciencedirect.com)

# Current Research in Pharmacology and Drug Discovery

journal homepage: [www.journals.elsevier.com/current-research-in-pharmacology-and-drug-discovery](http://www.journals.elsevier.com/current-research-in-pharmacology-and-drug-discovery)

## Inhibition of cotranslational translocation by apratoxin S4: Effects on oncogenic receptor tyrosine kinases and the fate of transmembrane proteins produced in the cytoplasm



Weijing Cai<sup>a,b,1</sup>, Ranjala Ratnayake<sup>a,b,1</sup>, Mengxiong Wang<sup>c</sup>, Qi-Yin Chen<sup>a,b</sup>, Kevin P. Raisch<sup>d,e</sup>, Long H. Dang<sup>b,f</sup>, Brian K. Law<sup>b,c</sup>, Hendrik Luesch<sup>a,b,\*</sup>

<sup>a</sup> Department of Medicinal Chemistry, College of Pharmacy, University of Florida, Gainesville, FL, 32610, USA

<sup>b</sup> Center for Natural Products, Drug Discovery and Development (CNPDD3), University of Florida, Gainesville, FL, 32610, USA

<sup>c</sup> Department of Pharmacology and Therapeutics, College of Medicine, University of Florida, Gainesville, FL, 32610, USA

<sup>d</sup> Department of Otolaryngology, College of Medicine, University of Florida, Gainesville, FL, 32610, USA

<sup>e</sup> College of Osteopathic Medicine, Lake Erie College of Osteopathic Medicine, Bradenton, FL, 34211, USA

<sup>f</sup> Department of Medicine, College of Medicine, University of Florida, Gainesville, FL, 32610, USA

### ARTICLE INFO

#### Keywords:

Sec61  
Cotranslational translocation  
N-glycosylation  
KRAS  
RTK inhibitors  
CDCP1

### ABSTRACT

Receptor tyrosine kinases (RTKs) have become major targets for anticancer therapy. However, resistance and signaling pathway redundancy has been problematic. The marine-derived apratoxins act complementary to direct kinase inhibitors by downregulating the levels of multiple of these receptors and additionally prevent the secretion of growth factors that act on these receptors by targeting Sec61 $\alpha$ , therefore interfering with cotranslational translocation. We have profiled the synthetic, natural product-inspired apratoxin S4 against panels of cancer cells characterized by differential sensitivity to RTK inhibitors due to receptor mutations, oncogenic KRAS mutations, or activation of compensatory pathways. Apratoxin S4 was active at low-nanomolar to sub-nanomolar concentrations against panels of lung, head and neck, bladder, and pancreatic cancer cells, concomitant with the downregulation of levels of several RTKs, including EGFR, MET and others. However, the requisite concentration to inhibit certain receptors varied, suggesting some differential substrate selectivity in cellular settings. This selectivity was most pronounced in breast cancer cells, where apratoxin S4 selectively targeted HER3 over HER2 and showed greater activity against ER<sup>+</sup> and triple negative breast cancer cells than HER2<sup>+</sup> cancer cells. Depending on the breast cancer subtype, apratoxin S4 differentially downregulated transmembrane protein CDCP1, which is linked to metastasis and invasion in breast cancer and modulates EGFR activity. We followed the fate of CDCP1 through proteomics and found that nonglycosylated CDCP1 associates with chaperone HSP70 and HUWE1 that functions as an E3 ubiquitin ligase and presumably targets CDCP1, as well as potentially other substrates inhibited by apratoxins, for proteasomal degradation. By preventing cotranslational translocation of VEGF and other proangiogenic factors as well as VEGFR2 and other receptors, apratoxins also possess anti-angiogenic activity, which was validated in endothelial cells where downregulation of VEGFR2 was observed, extending the therapeutic scope to angiogenic diseases.

### 1. Introduction

Cancer is a genetic disease, due to the progressive accumulation of mutations in oncogenes and tumor suppressor genes. In cancer, “driver” mutations lead to the constitutive activation of the mutant signaling protein which then induce and sustain tumorigenesis. For example, in

non-small cell lung cancer, “driver” mutations can occur in receptor tyrosine kinases (e.g., EGFR, HER2, MET, RET, ROS1) and downstream signaling proteins (e.g., AKT1, ALK, BRAF, KRAS, MEK1, NRAS, PIK3CA) (<https://www.mycancergenome.org/content/disease/non-small-cell-lung-carcinoma/>). In addition, amplification or overexpression of receptor tyrosine kinases like EGFR1-4, VEGFR1-3, MET and their growth factor

\* Corresponding author. Department of Medicinal Chemistry, College of Pharmacy, University of Florida, Gainesville, FL, 32610, USA.

E-mail address: [luesch@cop.ufl.edu](mailto:luesch@cop.ufl.edu) (H. Luesch).

<sup>1</sup> Contributed equally.

<https://doi.org/10.1016/j.crphar.2021.100053>

Received 28 July 2021; Received in revised form 7 August 2021; Accepted 1 September 2021

2590-2571/© 2021 The Authors. Published by Elsevier B.V. This is an open access article under the CC BY-NC-ND license (<http://creativecommons.org/licenses/by-nc-nd/4.0/>).

**Table 1**  
FDA approved drugs targeting growth factor receptors and growth factors.

Drug type	Drug	Disease indication	Molecular target <sup>a</sup>
Monoclonal antibody	Trastuzumab	Breast cancer	HER2
	Pertuzumab	Breast cancer	HER2
	Bevacizumab	Colorectal cancer (CRC)	VEGF
	Ramucirumab	Gastric cancer	VEGFR2
	Cetuximab	CRC with wild-type KRAS	EGFR
Kinase inhibitor	Panitumumab	CRC with wild-type KRAS	EGFR
	Imatinib	Leukemias, gastrointestinal, stromal tumor (GIST)	(BCR-ABL), c-KIT, PDGFRs
	Gefitinib	Non-small cell lung cancer (NSCLC)	EGFR
	Brigatinib	Anaplastic lymphoma, NSCLC	ALK, ROS1, IGF1R, FLT3, EGFR
	Dacomitinib	EGFR- mutated NSCLC	EGFR, HER2, HER4
	Neratinib	HER2+ breast cancer	HER2
	Osimertinib	NSCLC	EGFR T970M
	Erdaftinib	Urothelial carcinoma	FGFR1,2,3,4
	Erlotinib	NSCLC	EGFR
	Sorafenib	Renal cell cancer (RCC), hepatocellular carcinoma (HCC)	VEGFRs, PDGFRs, (B-RAF, MEK, ERK)
	Sunitinib	RCC, GIST	VEGFR2, PDGFR- $\beta$ , KIT, RET, CSF1R, FLT3
	Nilotinib	Chronic myelogenous leukemia (CML)	BCR-ABL, KIT, EPHA3,8, DDR1,2, (LCK)
	Dasatinib	CML, acute lymphocytic leukemia (ALL)	BCR-ABL, KIT, PDGFRs, EPHA2/B2, (CSK, SRC)
	Lapatinib	Breast cancer	EGFR, HER2
	Lenvatinib	Thyroid cancer, HCC, RCC	VEGFR2, 3
	Axitinib	RCC	VEGFRs, PDGFRs, KIT
	Afatinib	NSCLC, head and neck cancer, breast cancer	HER2, EGFR
	Crizotinib	NSCLC, anaplastic large cell lymphoma, neuroblastoma	MET
	Cabozantinib	Medullary thyroid cancer, HCC, RCC	VEGFR, MET, RET, TRKB, TIE2, AXL
	Pazopanib	RCC, soft tissue sarcoma	PDGFRs, VEGFRs
Ponatinib	CML, Philadelphia chromosome positive	PDGFRs, KIT, FGFR, VEGFRs, (SRC, BCR-ABL)	
Regorafenib	ALL, CRC	TIE2, PDGFRs, (B-RAF, MEK, ERK)	

<sup>a</sup> Non-RTK targets are given in parenthesis.

ligands also contribute to cancer progression (<https://www.mycancergenome.org/content/disease/non-small-cell-lung-carcinoma/>). There has been significant interest in developing drugs targeting receptor tyrosine kinases (RTKs), and downstream signaling proteins. These drugs include monoclonal antibodies and RTK inhibitors (Table 1). Due to

inherent redundancy in RTK signaling pathways and development of secondary mutations, drugs targeting one specific RTK or even multi-targeted RTKs have either been ineffective or quickly led to resistance. For example, treatment of lung cancer with the EGFR kinase inhibitor erlotinib showed both primary and secondary resistance due to the reactivation of downstream signaling pathways, through induction of parallel RTKs (MET, HER2, HER3, IGF1R, VEGFR) or secondary mutations in EGFR (T790M mutation) (Dienstmann et al., 2012; Suda et al., 2010; Tang et al., 2008; Bean et al., 2007). Resistance to treatment with the anti-EGFR monoclonal antibody cetuximab in head and neck cancer is due to constitutive activation of the HER3 RTK pathway (Harari et al., 2009; Jiang et al., 2014).

We discovered the apratoxin class of cytotoxic agents from marine cyanobacteria and determined that they prevent cotranslational translocation of secretory proteins, including receptor tyrosine kinases and their corresponding ligands, followed by proteasomal degradation of these proteins in the cytoplasm rather than export to the cell membrane or extracellular environment, respectively (Liu et al., 2009). Apratoxins act by directly targeting Sec61 $\alpha$  of the translocon in the endoplasmic reticulum membrane (Paatero et al., 2016). Synthesis and medicinal chemistry campaigns coupled with bioavailability and efficacy studies in cancer models established that synthetic analogues of the natural products, including apratoxins S4 and S10, have potent activity in various xenograft models for colon and pancreatic cancer (Chen et al., 2011, 2014; Cai et al., 2017; Cai et al., 2019), where oncogenic KRAS mutations are prevalent (32–57% and 72–90%, respectively) that negate the activity of direct RTK inhibitors acting upstream (Adjei, 2001; Prior et al., 2012). In addition to direct effect on cancer cells, apratoxins may also modulate the tumor microenvironment by inhibiting the secretion of certain pro-growth signaling factors from tumor-associated stromal cells (Cai et al., 2019). Our data suggested that apratoxins are complementary to existing drugs that act on either receptors (including RTKs) or growth factors (using antibodies). Based on the mechanism of action of apratoxins, we hypothesized that this compound class would be effective in cancers with activated growth factor receptor pathways, such as EGFR, VEGFR, MET and HER2/3, which include lung, head and neck, bladder, and breast cancers. Apratoxins are expected to also be effective in the subtypes that are resistant to currently available RTK inhibitors (Table 1), as they simultaneously downregulate a multitude of RTKs and the respective growth factors. In addition, apratoxins would also down-regulate mutated RTKs that are resistant to kinase inhibitors (e.g., EGFR T790M).

Inhibition of the secretory pathway is an innovative way to prevent export of receptors and secretory molecules from the cytoplasm, leading to receptor (including RTK) depletion and preventing secretion of the corresponding ligands, growth factors and cytokines (Luesch and Paavilainen, 2020). Based on our data, this one-two punch has unusually potent antiproliferative activity and may be an effective alternative to combination therapy with multiple (or broad-spectrum) RTK and growth factor inhibitors and additionally promises to have efficacy in cancers independent of KRAS status (Cai et al., 2017, 2019). Furthermore, the preclinical candidate apratoxin S10 exerted activity against cancer cells derived from highly vascularized tumors with 2000–5000 times greater

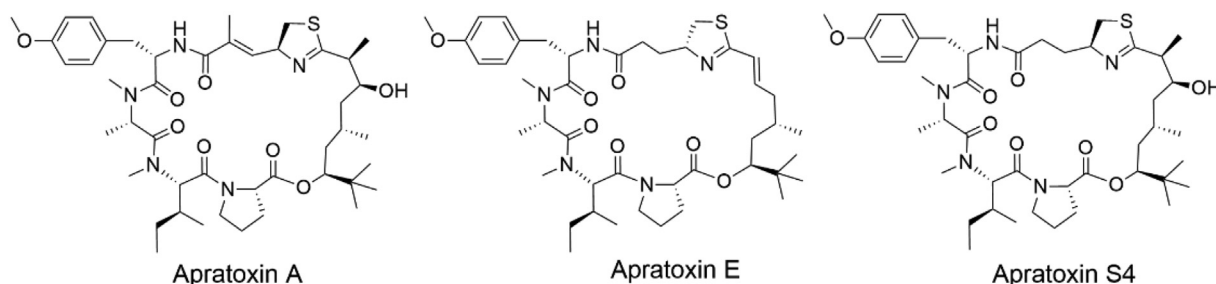


**Fig. 1.** Structures of natural apratoxins A and E and the synthetic analogue apratoxin S4.

potency than standard RTK inhibitors and also displayed antiangiogenic activity, in addition to its inherent anticancer properties (Cai et al., 2017). Due to the unique mechanism, inhibiting VEGF secretion and downregulating other proangiogenic factors and receptors, apratoxin S4 was recently “repurposed” and shown to be highly effective in inhibiting ocular angiogenesis, and specifically pathological neovascularization, in organoids, rabbit and mouse models, and acting on retinal endothelial cells as well as pericytes (Qiu et al., 2019). These data suggest that apratoxin S4 is also a treatment option to prevent blindness, even for populations that are resistant to anti-VEGF (standard-of-care) therapy.

NCI-60 data indicated that the natural product apratoxin A has broad-spectrum activity yet displayed a unique differential cytotoxicity profile (Luesch et al., 2006). The more recently discovered marine-derived inhibitor of cotranslational translocation, coibamide A, has a distinct cytotoxicity profile, despite sharing the same target as apratoxins, Sec61 $\alpha$  (Tranter et al., 2020). These pharmacological nuances between these agents might be due to the targeting of different Sec61 $\alpha$  sites, leading to a unique cellular fingerprint (Luesch and Paavilainen, 2020). In fact, Sec61 $\alpha$  mutants resistant to apratoxin A were different from the resistance profile of all other known Sec61 $\alpha$  targeting agents, providing support for the distinctive activity of the apratoxin class family (Luesch and Paavilainen, 2020). Here we profiled the broad-spectrum activity of preclinical candidate apratoxin S4 (Chen et al., 2011), a synthetic analogue inspired by the natural products apratoxins A and E (Fig. 1) (Luesch et al., 2001; Matthew et al., 2008; Wu et al., 2016), across cell types with respect to antiproliferative activity, relevant RTK substrates for cotranslational translocation, and deciphered cell type dependent differences in breast cancer panels. We also provided deeper insight into the fate and potential mechanism of degradation of secretory proteins induced by apratoxin S4.

## 2. Materials and methods

### 2.1. Synthesis

Apratoxin S4 was synthesized as previously described (Chen et al., 2014).

### 2.2. Cell culture

Breast, lung and bladder cancer cells, as well as the epidermoid carcinoma A431 cells and the PANC-1 pancreatic cancer cells, were purchased from the American Type Culture Collection (ATCC) in Baltimore (MD) or Manassas (VA). Human Umbilical Vein Endothelial Cells (HUVEC, cat# CC-2519) were purchased from Lonza. QGP1 pancreatic carcinoma cells were purchased from the Japanese Cancer Research Resources Bank (JCRB; cat#: JCRB0183).

The Breast panel cells, as well as PANC-1 and RT4 cells were propagated in Dulbecco's Minimum Essential Medium (DMEM) supplemented with 10% fetal bovine serum (FBS), 10 Units/mL penicillin, 100  $\mu$ g/mL streptomycin and 250 ng/mL amphotericin B. T24 bladder cancer cells were grown in Eagle's Minimum Essential Medium (EMEM) supplemented with 10% fetal bovine serum (FBS), 10 Units/mL penicillin, 100  $\mu$ g/mL streptomycin and 250 ng/mL amphotericin B. The lung cancer panel cells, as well as QGP-1 and SW780 cells were cultured in RPMI-1640 medium supplemented with 10% fetal bovine serum (FBS), 10 Units/mL penicillin, 100  $\mu$ g/mL streptomycin and 250 ng/mL amphotericin B. A-431 cells were grown in DMEM:F12 (50:50) media supplemented with 15% FBS, L-glutamine, penicillin and streptomycin. HUVEC cells were cultured in EGM (Lonza cat# CC-3124).

A panel of 5 cell lines of head and neck origin and 1 cell line of gynecological origin were used in this study. The head and neck cell lines, UM-SCC-1, UM-SCC-5, UM-SCC-6, UM-SCC-38 and UM-SCC-47 (Grénman et al., 1991; Brenner et al., 2010) were generously provided by Thomas Carey (University of Michigan, Ann Arbor, MI). The UM-SCC cell lines were maintained in DMEM supplemented with 1%

non-essential amino acids, 2 mmol/L L-glutamine, penicillin and streptomycin and 15% fetal bovine serum (FBS). All cell lines were cultured at 37 °C in 5% CO<sub>2</sub>.

### 2.3. Cell viability assays

Cells were seeded in a 96-well clear bottom plate and after 24 h treated with various concentrations of apratoxin S4 or solvent control (EtOH). After 48 h of incubation, cancer cell viability was detected using MTT according to the manufacturer's instructions (Promega, Madison, WI). For HUVECs, cell viability was measured after 14 h. Nonlinear regression analysis was carried out using GraphPad Prism software.

### 2.4. Immunoblot analysis

Cells were seeded in 6-well clear bottom plates the day before treatment. The next day, cells were treated with apratoxin S4 or solvent control (EtOH). 24 h later, whole cell lysates were collected using PhosphoSafe buffer (EMD Chemicals, Inc, Gibbstown, NJ). Protein concentrations were measured with the BCA Protein Assay kit (Thermo Fisher Scientific, Rockford, IL). Lysates containing equal amounts of protein were separated by SDS polyacrylamide gel electrophoresis (4–12%), transferred to polyvinylidene difluoride membranes, probed with primary and secondary antibodies, and detected with the Super-Signal West Femto Maximum Sensitivity Substrate (Thermo Fisher Scientific). Anti-VEGFR2 (2479S), EGFR (2232S), MET (3148S), IGF1R $\beta$  (3027S), HER2 (2165), HER3 (4754), survivin (2808), CDCP1 (13794),  $\beta$ -actin (4970S) and secondary anti-mouse and rabbit antibodies were obtained from Cell Signaling Technology, Inc (Danvers, MA) and RET antibody (ab134100) was obtained from Abcam (Cambridge, MA). Bands shown in the immunoblots were observed in the expected molecular weight range.

### 2.5. Angiogenesis assay

HUVECs (Lonza) were used at passage 4 for this assay. In vitro Angiogenesis Assay Kit (Chemicon) was used according to the manufacturer's recommendation. Briefly, an ice-cold mixture of ECMatrix (50  $\mu$ L per well) was transferred into a precooled 96-well plate. After the matrix solution had solidified (>1 h incubation at 37 °C), 23,000 cells were mixed with the appropriate inhibitor concentration (in 100  $\mu$ L EGM) and plated into each well. After incubation at 37 °C for 14 h, images were captured for each well using a Nikon inverted microscope equipped with NIS-Elements software. Branch point counting was used as quantification method. Five random microscope view-fields were counted and the number of branch points was averaged. The number of junctions were analyzed by the Angiogenesis Analyzer plug-in for ImageJ (n = 5 per group).

### 2.6. CDCP1 proteomics studies

Identification of CDCP1-associated proteins was carried out essentially as described previously (Law et al., 2013; 2016). Briefly, T47D cells were infected with adenoviruses encoding GFP or Flag-CDCP1 and incubated for 24 h. The cells were then treated for 24 h with vehicle or 100 nM apratoxin and incubated for an additional 24 h. Cell extracts were prepared and subjected to immunoprecipitation with anti-Flag-Agarose (Sigma-Aldrich, St. Louis, Mo.), followed by elution with Flag peptide as described previously (Law et al., 2013; 2016). Eluted proteins were concentrated by precipitation with 10% trichloroacetic acid, separated by SDS-PAGE, stained with colloidal Coomassie, and bands of interest were excised and submitted to the University of Florida Interdisciplinary Center for Biotechnology Research (ICBR) Proteomics Core for analysis as described previously (Law et al., 2013; 2016). Briefly, samples were reduced, alkylated with Iodoacetamide and digested with Trypsin. The tryptic digests were injected onto a capillary trap (LC

**Table 2**  
Human cancer cell lines tested in this study and their characteristics.

Cancer type	Cell line	EGFR inhibitor sensitivity	Characteristics	
Lung	NCI-H1975	Erlotinib resistant	EGFR mutation T790M	
	A549	Erlotinib resistant	EGFR wild-type, KRAS mutated, G12S, MET activated	
	NCI-H358	Erlotinib resistant	EGFR wild-type, IGF-1R activated	
	NCI-H1650	Gefitinib/erlotinib resistant	EGFR mutation exon 19 deletion, PTEN deleted, IGF-1R activated	
	NCI-H727	Erlotinib resistant	EGF expression, KRAS mutated, G12V	
	Head & Neck	A431	Cetuximab resistant	High EGFR expression
		UM-SCC-1	Cetuximab resistant	Low EGFR expression
UM-SCC-5		Cetuximab moderately sensitive	Moderate EGFR expression	
UM-SCC-6		Cetuximab sensitive	High EGFR expression	
UM-SCC-38		Gefitinib sensitive	Low EGFR expression, high HER2, HER3 expression	
UM-SCC-47		Cetuximab resistant	High EGFR expression, HER3 activated	
Bladder		RT4	Gefitinib resistant	High EGFR expression, activated FGFR3 (FGFR3-TACC3 fusion)
	SW780		Activated FGFR3 (FGFR3-BAIAP2L1 fusion), high MET expression	
	T24		FGFR3 wild-type, high MET expression	
Pancreas	PANC-1	Erlotinib resistant	KRAS mutated, G12D	
	QGP-1	Erlotinib resistant	KRAS mutated, G12V	
Breast	MDA-MB-436		Triple negative, BRCA1 mutated	
	MDA-MB-468	Gefitinib resistant	Triple negative, BRCA1 WT, amplified EGFR	
	MCF-7		ER/PR positive	
	T47D		ER/PR positive	
	BT474		ER/PR positive, HER2 positive	

Packings PepMap, Thermo Fisher Scientific) and washed for 5 min with a flow rate of 5  $\mu$ L/min of 0.1% v/v acetic acid. The samples were loaded onto an LC Packing® C18 Pep Map HPLC column and eluted with a gradient starting from 97% solvent A, 3% solvent B and finishing at 40% solvent A, 60% solvent B. Solvent A consisted of 0.1% v/v acetic acid, 3% v/v acetonitrile (ACN), and 96.9% v/v H<sub>2</sub>O. Solvent B consisted of 0.1% v/v acetic acid, 96.9% v/v ACN, and 3% v/v H<sub>2</sub>O. The flow rate was 300 nL/min and LC-MS/MS analysis was carried out on a hybrid quadrupole-TOF mass spectrometer (QSTAR Elite, AB Sciex Inc., Framingham, MA, USA). The focusing potential and ion spray voltage were set to 275 V and 2400 V, respectively. The information-dependent acquisition (IDA) mode of operation was employed in which a survey scan from *m/z* 400–1200 was acquired followed by collision-induced dissociation (CID) of the four most intense ions.

### 2.7. Database searching

All MS/MS samples were analyzed using Mascot (Matrix Science, London, UK; version 2.2.07). Mascot was set up to search the IPI\_human\_20120411 database assuming the digestion enzyme trypsin. Mascot was searched with a fragment ion mass tolerance of 0.50 Da and a parent ion tolerance of 0.50 Da. Iodoacetamide derivative of cysteine was specified in Mascot as a fixed modification. S-carbamoylmethylcysteine cyclization (N-terminus), deamidation of asparagine and glutamine and oxidation of methionine were specified in Mascot as variable modifications.

### 2.8. Criteria for protein identification

Scaffold (version Scaffold\_4.11.0, Proteome Software Inc., Portland, OR) was used to validate MS/MS based peptide and protein identifications. Peptide identifications were accepted if they could be established at greater than 90.0% probability by the Peptide Prophet algorithm (Keller et al., 2002). Protein identifications were accepted if they could be established at greater than 99.0% probability and contained at least 2 identified peptides. Protein probabilities were assigned by the Protein Prophet algorithm (Nesvizhskii et al., 2003). Proteins that contained similar peptides and could not be differentiated based on MS/MS analysis alone were grouped to satisfy the principles of parsimony.

## 3. Results and discussion

### 3.1. Cellular profiling of apratoxin S4 against various types of cancer cells, including KRAS mutant cells and others with differential sensitivity to RTK inhibitors

We previously showed that apratoxin S4 has potent antiproliferative activity against HCT116 human colon cancer cells in vitro, concomitant with MET downregulation, and efficacy in a HCT116 xenograft model in vivo (Chen et al., 2011; 2014). HCT116 cells are characterized by KRAS mutations, including G13D, and others (Alves et al., 2015), yet apratoxin S4 displayed excellent activity. We then profiled apratoxin S4 against panels of cancer cell lines to obtain a more comprehensive view of the anticancer potential of the compound and extend its potential applicability towards treating other cancers. We selected panels of lung, head and neck, bladder, pancreas, and breast cancer cell lines with differential sensitivity to RTK inhibitors due to aberrant expression of EGFR, MET or other receptors, or due to KRAS mutations (Table 2). Apratoxin S4 was effective against almost all of these cell lines, regardless of receptor levels, although efficacy varied. Specifically, apratoxin S4 showed potent and broad-spectrum antiproliferative activities against lung, head and neck, and bladder cancer cell panels (Fig. 2A). The activity largely correlated with the downregulation of multiple RTKs, including EGFR and MET, with effects around 1–10 nM, when maximum efficacy was reached in the corresponding cell type (Fig. 2B).

The initial cellular profiling at log-fold dilutions already hinted at the differential downregulation of different receptors in different cell types. For example, in the lung panel, levels of EGFR, MET, VEGFR2, and PDGFR- $\beta$  were attenuated at different concentrations, suggestive of substrate specificity in cells, even though apratoxin A was previously determined to prevent cotranslational translocation in a substrate-independent manner (Paatero et al., 2016). Nevertheless, in cells the selectivity becomes apparent, as we had previously hypothesized (Chen et al., 2011; Luesch and Paavilainen, 2020). In H1975 cells, PDGFR- $\beta$  appeared to be the most sensitive substrate among those four tested (Fig. 2B).

In head and neck cancer cell panel, EGFR was consistently downregulated across all cell types at 10 nM; however, the sensitivity of MET was variable, with greatest sensitivity in A431 cells. No particular trend was determined in bladder cells.

We then performed a more detailed dose-response analysis using half-log concentrations in NCI-H727 lung cancer cells that also have mutated KRAS (Fig. 3A and B). As expected, we found potent antiproliferative activity in the low nM range and that several RTKs (substrates for cotranslational translocation) are downregulated in this cellular context as well. Intriguingly, while EGFR and IGF1R $\beta$  are almost completely depleted at 1 nM, it required 10 nM to eliminate functional (glycosylated) VEGFR2 (Fig. 3B). The exocrine pancreatic cancer cell line PANC-1 and pancreatic neuroendocrine tumor cells QGP-1 were also inhibited in the same concentration range, although with comparatively reduced efficacy (Fig. 3C). In PANC-1 cells, EGFR and VEGFR2 were inhibited near 320 pM compared with 1 nM for IGF1R $\beta$  (Fig. 3D). In QGP-1 cells, both tested substrates for cotranslational translocation that showed an

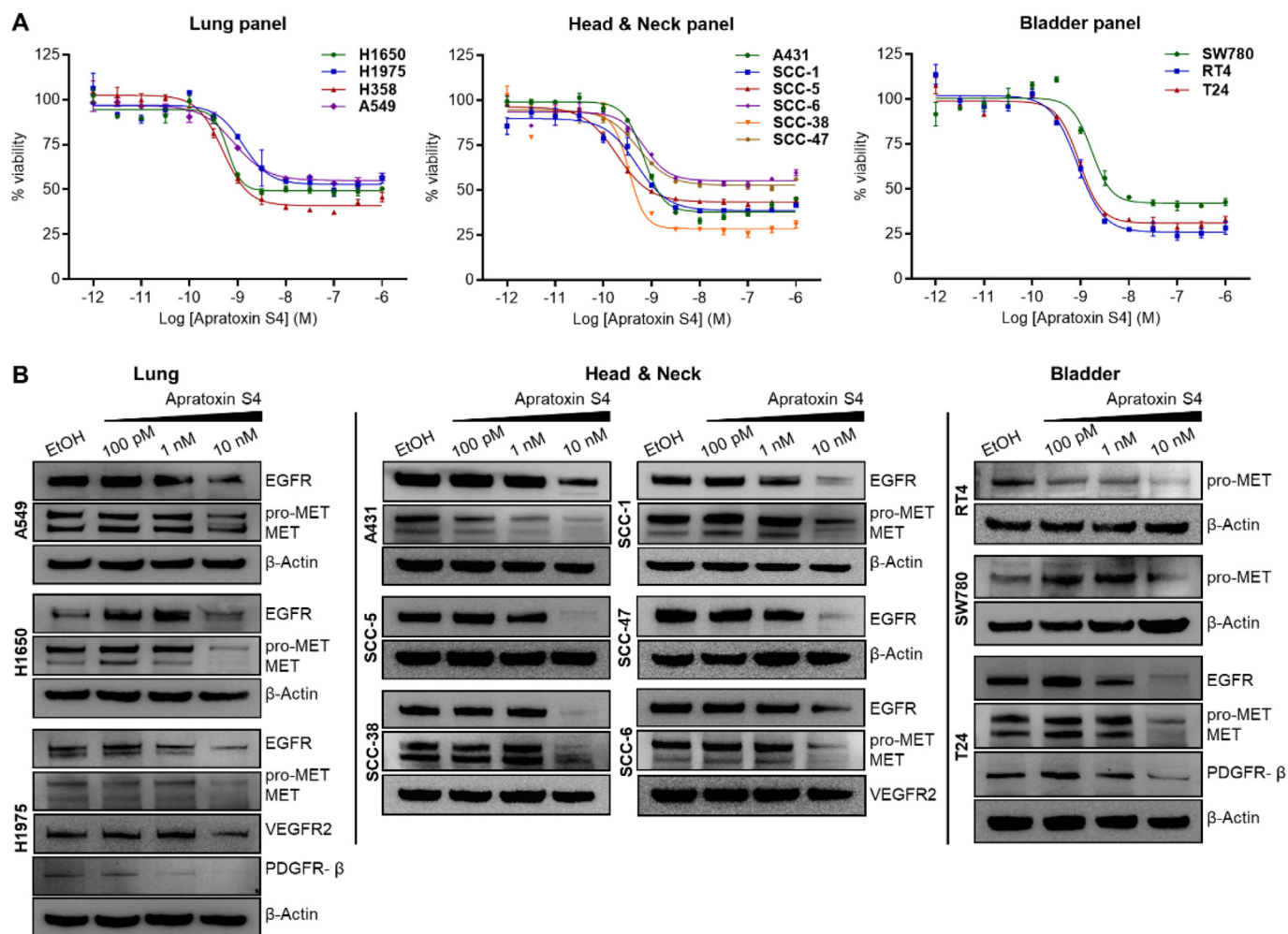


**Fig. 2.** Effects of apratoxin S4 on various lung, head and neck, and bladder cancer cell lines (see Table 2). (A) Dose-response analysis in the MTT cell viability assay (48 h). Error bars indicate mean  $\pm$  SD of three replicates (B) Dose-dependent downregulation of selected RTKs monitored by Western blot analysis (24 h).

immunoreactive band by Western blot (RET and IGF1 $\beta$ ) were inhibited equally ( $\sim$ 3.2 nM, Fig. 3D). The potent activity of apratoxin S4 against cells with mutant (including oncogenic) KRAS indicates that KRAS requires additional proteins that go through the secretory pathway. Based on the compression of the dose-response curve, the efficacy of apratoxin S4 against pancreatic cancer cells is lower yet potency is high. This is suggestive of growth inhibition rather than cytotoxicity, as described for apratoxin S10 (Cai et al., 2019).

With respect to clinical impact, overall these findings suggest that apratoxin S4 has efficacy in a KRAS mutant background, where RTK inhibitors are ineffective. In general, RTKs may be used as biomarkers to predict efficacy and responses. Furthermore, subtle differential substrate sensitivities suggest that profiles might be tunable using the apratoxin scaffold.

### 3.2. Differential sensitivity and efficacy of apratoxin S4 in different subtypes of breast cancer cells

Breast cancer is classified into four subtypes: triple negative (Estrogen Receptor (ER) negative, Progesterone (PR) negative, HER2 negative), Luminal A (ER positive, PR positive, and HER2 negative), Luminal B (ER positive, PR positive, HER2 positive) and HER2 enriched (ER negative, PR negative, HER2 positive). Luminal A breast cancer cells (MCF7 and T47D) were the most sensitive breast cancer cell type to apratoxin S4; less than 40% of the cells remained viable. Triple negative cells (MDA-MB-436 and MDA-MB-468) showed moderate sensitivity. After treatment

with apratoxin S4 for 48 h, more than 70% cell viability was observed in Luminal B cells (BT474) (Fig. 4A).

Given the interesting differential response of apratoxin S4 against different types of breast cancer cells, we aimed to investigate the potential mechanisms involved. Since apratoxin S4 downregulated multiple RTKs in other sensitive cancer cell types, we questioned whether the differential sensitivity against breast cancer cells is due to its RTK substrate selectivity and if there is a clear pattern. EGFR was consistently downregulated (Fig. 4B–E). However, the results supported our hypothesis as HER3 was downregulated in all cell types, while HER2 was downregulated in T47D but not BT474 (Fig. 4C,E). In agreement with our findings, a similar effect with higher relative sensitivity of HER3 compared to HER2 was also observed recently with apratoxin A and another Sec61 inhibitor, coibamide A, although in that study apratoxin A showed slight dose-dependent inhibition of HER2 in BT474 as well (Kazemi et al., 2021). Downregulation of these receptors was associated with decreased expression of the anti-apoptotic protein survivin (Fig. 4C and D). The lack of downregulation of HER2 in BT474 cells may explain the low efficacy of apratoxin S4 against BT474 cells, which are HER2 and ER positive and stopping these cells requires inhibition of both ER and HER2. Clearly, apratoxin S4 can discriminate between HER2 and HER3 in breast cancer cells and exhibits a pronounced preference. However, this selectivity is not only substrate dependent but also cell type dependent: HER2 was previously shown to be strongly downregulated by apratoxin A in U2OS osteosarcoma (Liu et al., 2009) cells but almost unaffected in breast cancer cells. The data suggest that apratoxin S4

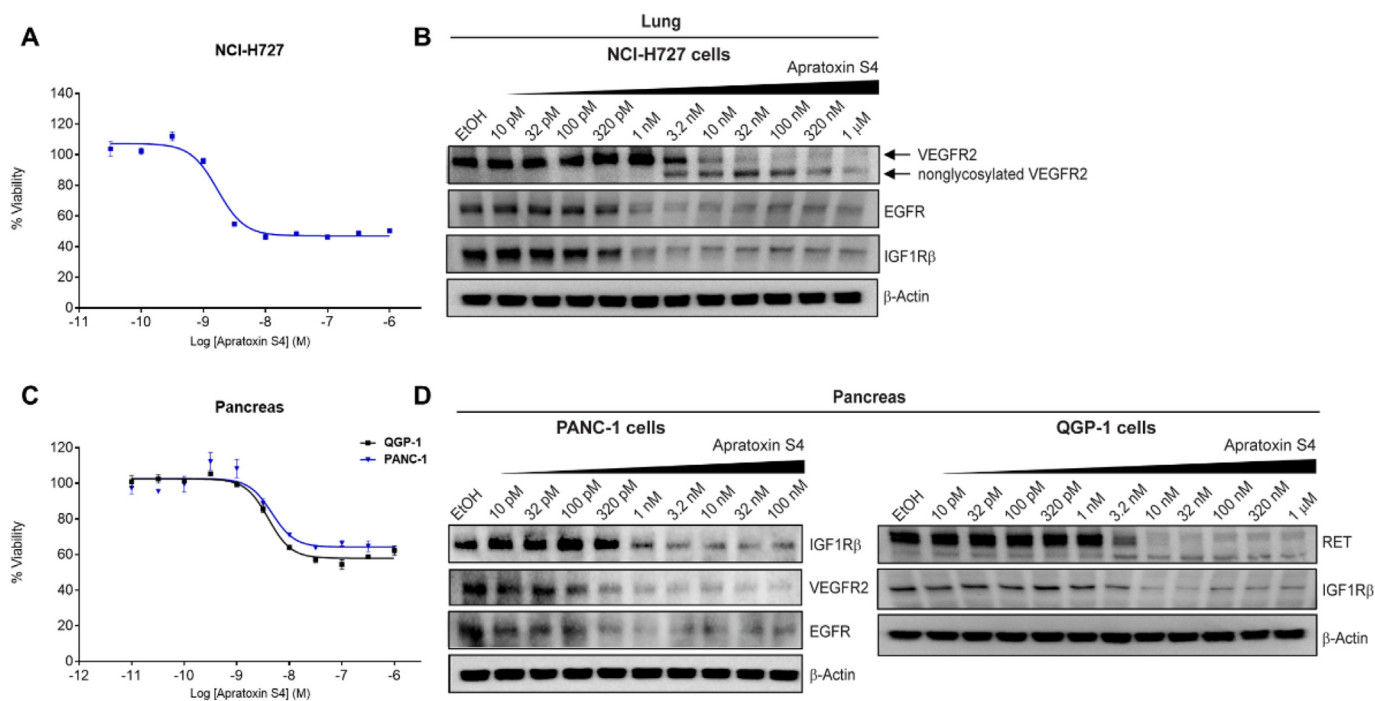


**Fig. 3.** Activity of apratoxin S4 against selected pancreatic cancer and lung cancer cells. Apratoxin S4 downregulates multiple RTKs in these cancer cell lines near the effective concentration that reduces cell viability. (A,C) Dose-response analysis in the MTT cell viability assay (48 h). Error bars indicate mean ± SD of three replicates (B,D) Dose-dependent downregulation of selected RTKs monitored by Western blot analysis (24 h).

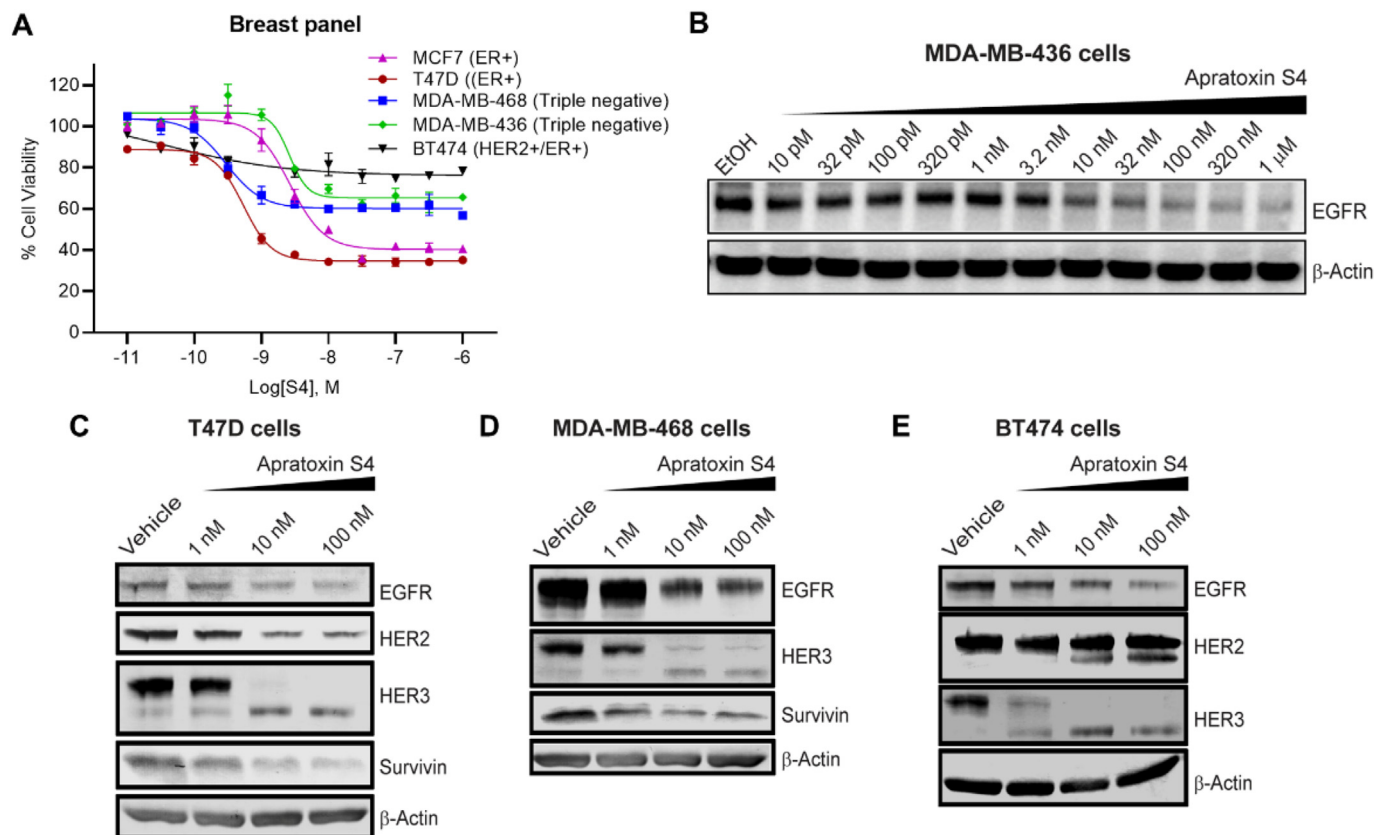


**Fig. 4.** Activities of apratoxin S4 against breast cancer cells. (A) Cell viability assay using MTT (48 h). Error bars indicate mean ± SD of three replicates (B–E) Apratoxin S4 selectively downregulates RTKs in breast cancer cells (24 h).

might be a suitable candidate for combination therapy with HER2 inhibitors/antibodies where HER3 activation is problematic with respect

to drug resistance. Therefore, cell type dependent selectivity profiles of apratoxin S4 coupled with cancer resistance profiles may guide rational

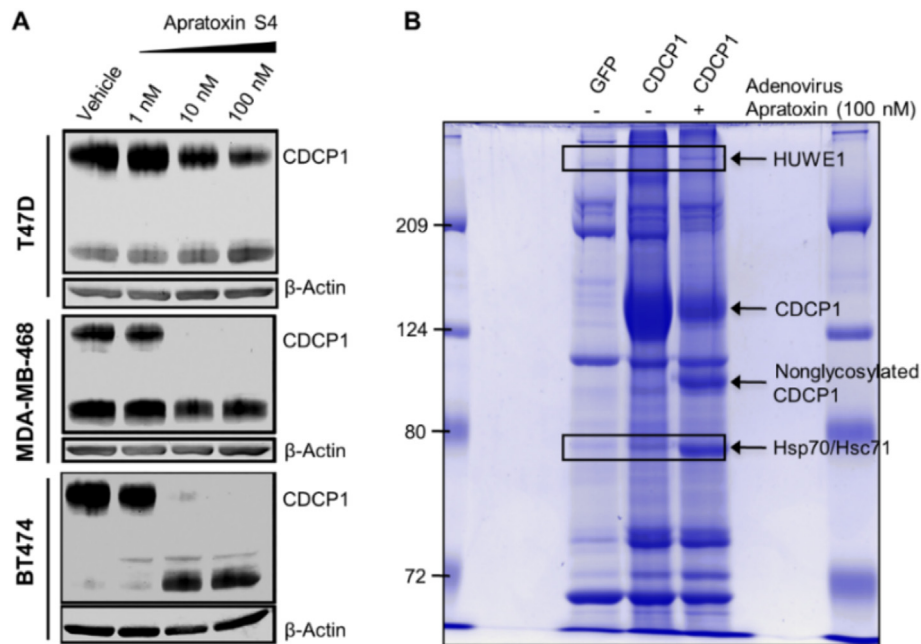


**Fig. 5.** Effects of apratoxin S4 and levels and fate of CDCP1. (A) CDCP1 was downregulated in breast cancer cells (24 h). (B) Proteomics analysis conducted in T47D cells (24 h treatment, 100 nM) indicated association of nonglycosylated CDCP1 with HSP70 and HUWE1.

combination therapies with RTK inhibitors to overcome drug resistance. Overall, and in general, the data articulate the intriguing complexity of inhibition of cotranslational translocation and that there are strong cell-type dependent preferences for different substrates. The differences in signal peptide sequence of cotranslational translocation substrates are insufficient to explain these results and the cellular context has to be taken into consideration. Interestingly, the substrate-specific Sec61 inhibitor cotransin showed a similar profile in breast cancer cells, indicating that both compounds possess inherent selectivity (Ruiz-Saenz et al., 2015).

### 3.3. Other non-RTK targets linked to migration and invasion

CDCP1 is a transmembrane protein linked to metastasis and invasion of breast cancer cells and forms a complex with EGFR that decreases cell adhesion (Law et al., 2013; 2016). CDCP1 is also a node in tumorigenic and metastatic signaling pathways in other cancer cell types (Khan et al., 2021) and is activated by oncogenic KRAS (Uekita et al., 2014). CDCP1 undergoes glycosylation and disulfide bonding during its transit through the secretory pathway. We had previously identified dexamethasone as an indirect inhibitor of CDCP1 processing, preventing the generation of the proinvasive cleaved form of CDCP1 (Law et al., 2013), which

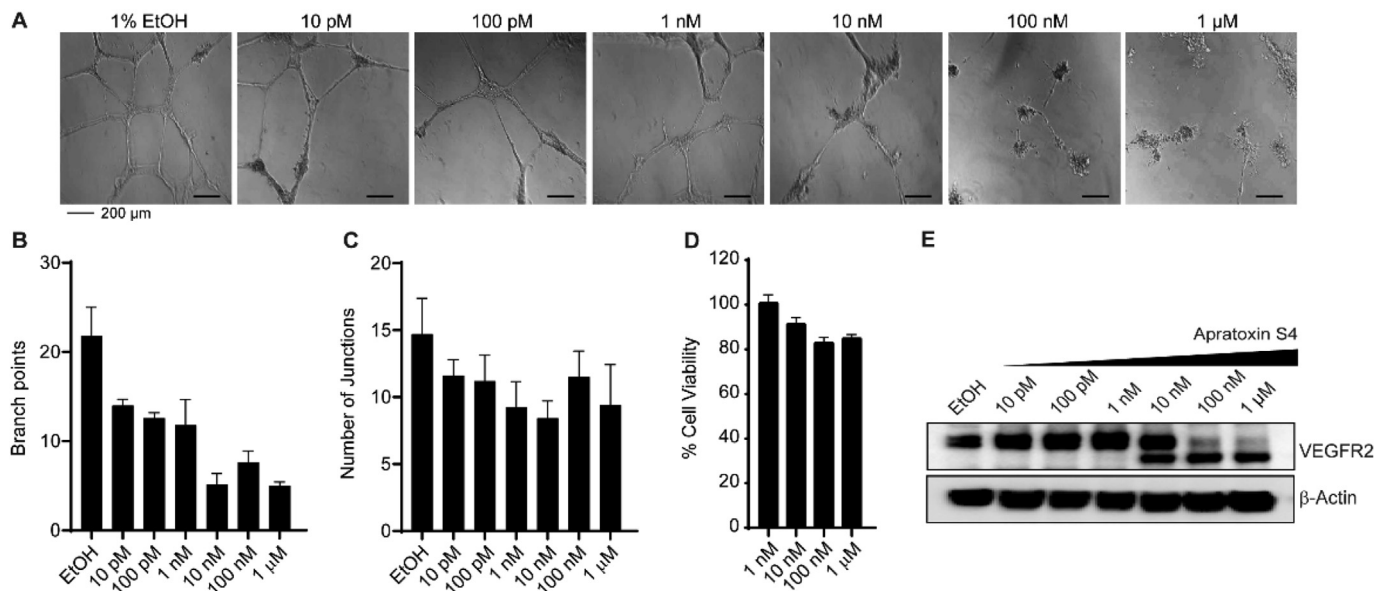


**Fig. 6.** Effects of apratoxin S4 in HUVEC angiogenesis model. (A) Apratoxin S4 inhibited angiogenesis in vitro in a dose-dependent manner, determined by Matrigel assay using HUVECs (scale bar 200 μm), 14 h. (B) Branch point counting was used as the quantification method. Five random microscope view-fields were counted and the number of branch points was averaged. (C) The number of junctions was analyzed by the Angiogenesis Analyzer plug-in for ImageJ (n = 5 per group). Error bars in (B) and (C) indicate mean + SEM of five fields. (D) Antiproliferative effect of apratoxin S4 on HUVECs. Error bars indicate mean + SD of three replicates. (E) Immunoblot analysis using lysates from apratoxin S4-treated HUVECs (14 h).

cooperates with the cyanobacterial class I HDAC inhibitor largazole to inhibit invasion and migration of breast cancer cells. Subsequently, we discovered the marine cyanobacterial serine protease inhibitor kempopeptin C, which inhibits plasmin and matriptase implicated in CDCP1 cleavage and activation, leading to inhibition of migration of TNBC cells (Al-Awadhi et al., 2017). Here we show that apratoxin S4 downregulates the full-length form of CDCP1 in three different breast cancer cell lines investigated, at 10 or 100 nM (Fig. 5A). In order to understand how apratoxin treatment alters CDCP1 processing, we performed affinity purification of Flag-CDCP1 from T47D cells treated with or without apratoxin and conducted proteomic analysis. In addition to observing nonglycosylated CDCP1 because of the lack of cotranslational translocation, compared with control pulldowns, new bands appeared corresponding to the chaperone HSP70 and the protein HUWE1 (Fig. 5B). The increased HSP70 association likely resulted from association with cytoplasmic, misfolded CDCP1. We speculate that HSP70 may play a similar role in chaperoning other apratoxin S4-induced aggregates for degradation. HUWE1 was detected with 100% probability from seven unique HUWE1 peptides. HUWE1 is a cytoplasmic protein that contains a Homologous E6-AP Carboxyl Terminus (HECT) domain that functions as an E3 ubiquitin ligase (Giong et al., 2020). HUWE1 ubiquitinates a number of proteins including the BCL2-related anti-apoptotic MCL1 protein, p53 tumor suppressor, histones and DNA polymerase beta for subsequent degradation (Giong et al., 2020; Kunz et al., 2020; Sing et al., 2021). Our data suggest that HUWE1 might also target CDCP1 for degradation in response to apratoxin treatment and potentially other substrates for which cotranslational translocation is blocked by apratoxins. It is also an intriguing possibility that apratoxins may recruit this E3 ligase in a targeted fashion, which remains to be tested.

### 3.4. Apratoxin S4 downregulates VEGFR2 in HUVEC angiogenesis model

We have recently shown that apratoxin S4 strongly inhibits retinal vascular cell activation by suppressing several angiogenic pathways (Qiu et al., 2019). It was shown to act on retinal endothelial cells as well as pericytes and has the potential to overcome drug resistance to anti-VEGF therapy through its unique mechanism of action (Qiu et al., 2019). Consistently and similar to apratoxin S10 (Cai et al., 2017), apratoxin S4 inhibited tube formation in a human umbilical vein endothelial cell (HUVEC) in vitro model (Fig. 6A). Branch point reduction in Matrigel was already seen starting at 10 pM and more severely reduced at higher concentrations (Fig. 6B). The number of junctions was also reduced in a concentration-dependent manner but to a much lesser extent (Fig. 6C). These effects occurred within 14 h without cytotoxicity (Fig. 6D). Therefore, in addition to its inherent anticancer properties, apratoxin S4 has potent antiangiogenic effects in multiple models through on-target pharmacological activity. Consequently, apratoxin S4 and related analogues are predicted to have benefits for the treatment of vascularized tumors, including renal cell carcinoma, hepatocellular carcinoma and neuroendocrine carcinoma (Cai et al., 2017), especially in settings of resistance to specific antiangiogenic therapy. Additionally, through manageable toxicity, these compounds also have non-cancer applications where angiogenesis plays a role.

## 4. Conclusions

Apratoxin S4 has potent activity in multiple cancer and normal cell types, enabling applications in different therapeutic settings. We have shown that apratoxin S4 is effective against a broad array of cancer cells, including those resistant to selective RTK inhibitors. Apratoxin S4 acts as an indirect RTK inhibitor and additionally prevents the trafficking from the cytoplasm to the ER of other secretory proteins, including RTK ligands, which leads to the modulation of multiple RTK signaling pathways. Contrary to EGFR inhibitors, apratoxin S4 has antiproliferative activity in a mutant KRAS background, extending its application to overcoming resistance to selective anticancer drugs. Furthermore, tumor

type-dependent and perhaps even patient-specific fingerprint secretion and selectivity profiles of apratoxin S4 may be predictive of responsive patient populations and guide personalized clinical investigations and rational combination therapies with RTK inhibitors and other agents. The inhibitory effects on tumor-associated stromal cells that secrete factors to drive pancreatic cancer cell growth had already been established for apratoxin S10, extending the mechanism beyond the direct activity on cancer cells. Apratoxin S4 also inhibits secretion in normal cells, providing opportunities to modulate the tumor microenvironment and inhibiting pathological angiogenesis. The complex interplay that leads to the observed cell type-dependent substrate selectivity and the potential role of Sec61-independent protein synthetic pathways are particularly intriguing. Which factors govern these effects remains to be elucidated and may guide modulation and further therapeutic application of apratoxins. Selective targeting of HER3 over HER2 in breast cancer cells suggest the potential of apratoxin S4 to be used in combination with HER2 therapy in refractory breast cancer.

## Funding

This research was supported by the NIH, National Cancer Institute Grants R01CA172310 (to H.L.) and R50CA211487 (to R.R.), and the Debbie and Sylvia DeSantis Chair professorship (H.L.).

## CRediT authorship contribution statement

**Weijing Cai:** Methodology, Formal analysis, Writing – original draft. **Ranjala Ratnayake:** Methodology, Formal analysis, Data curation, Writing – review & editing. **Mengxiang Wang:** Methodology, Formal analysis. **Qi-Yin Chen:** chemical synthesis of apratoxin S4. **Kevin P. Raisch:** Resources. **Long H. Dang:** Writing – review & editing, clinical input. **Brian K. Law:** Investigation, Resources, Writing – review & editing, Supervision. **Hendrik Luesch:** Conceptualization, Investigation, Resources, Writing – writing, review & editing, Project administration, Funding acquisition.

## Declaration of competing interest

The authors declare the following financial interests/personal relationships which may be considered as potential competing interests: H. Luesch is co-founder of Oceanyx Pharmaceuticals, Inc., which has licensed patents and patent applications related to the subject matter.

## Acknowledgments

We thank Sixue Chen, Director of the UF ICBR Proteomics Core, for performing the analysis of the proteomics data and Thomas Carey (University of Michigan) for providing the head and neck UM-SSC lines.

## References

- Adjei, A.A., 2001. Blocking oncogenic Ras signaling for cancer therapy. *J. Natl. Cancer Inst.* 93, 1062–1074.
- Al-Awadhi, F.H., Salvador, L.A., Law, B.K., Paul, V.J., Luesch, H., 2017. Kempopeptin C, a novel marine-derived serine protease inhibitor targeting invasive breast cancer. *Mar. Drugs* 15, 290.
- Alves, S., Castro, L., Fernandes, M.S., Francisco, R., Castro, P., Priault, M., Chaves, S.R., Moyer, M.P., Oliveira, C., Seruca, R., et al., 2015. Colorectal cancer-related mutant KRAS alleles function as positive regulators of autophagy. *Oncotarget* 6, 30787–30802.
- Bean, J., Brennan, C., Shih, J.Y., Riely, G., Viale, A., Wang, L., Chitale, D., Motoi, N., Szoke, J., Broderick, S., et al., 2007. MET amplification occurs with or without T790M mutations in EGFR mutant lung tumors with acquired resistance to gefitinib or erlotinib. *Proc. Natl. Acad. Sci. U.S.A.* 104, 20932–20937.
- Brenner, J.C., Graham, M.P., Kumar, B., Saunders, L.M., Kupfer, R., Lyons, R.H., Bradford, C.R., Carey, T.E., 2010. Genotyping of 73 UM-SCC head and neck squamous cell carcinoma cell lines. *Head Neck* 32, 417–426.
- Cai, W., Chen, Q.-Y., Dang, L.H., Luesch, H., 2017. Apratoxin S10, a dual inhibitor of angiogenesis and cancer cell growth to treat highly vascularized tumors. *ACS Med. Chem. Lett.* 8, 1007–1012.

- Cai, W., Ratnayake, R., Gerber, M.H., Chen, Q.-Y., Yu, Y., Derendorf, H., Trevino, J.G., Luesch, H., 2019. Development of apratoxin S10 (Apra S10) as an anti-pancreatic cancer agent and its preliminary evaluation in an orthotopic patient-derived xenograft (PDX) model. *Invest. New Drugs* 37, 364–374.
- Chen, Q.-Y., Liu, Y., Cai, W., Luesch, H., 2014. Improved total synthesis and biological evaluation of potent apratoxin S4 based anticancer agents with differential stability and further enhanced activity. *J. Med. Chem.* 57, 3011–3029.
- Chen, Q.-Y., Liu, Y., Luesch, H., 2011. Systematic chemical mutagenesis identifies a potent novel apratoxin A/E hybrid with improved in vivo antitumor activity. *ACS Med. Chem. Lett.* 2, 861–865.
- Dienstmann, R., de Dosso, S., Felip, E., Tabernero, J., 2012. Drug development to overcome resistance to egfr inhibitors in lung and colorectal cancer. *Mol. Oncol.* 6, 15–26.
- Gong, X., Du, D., Deng, Y., Zhou, Y., Sun, L., Yuan, S., 2020. The structure and regulation of the E3 ubiquitin ligase HUWE1 and its biological functions in cancer. *Invest. New Drugs* 38, 515–524.
- Grénman, R., Carey, T.E., McClatchey, K.D., Wagner, J.G., Pekkola-Heino, K., Schwartz, D.R., Wolf, G.T., Lacivita, L.P., Ho, L., Baker, S.R., et al., 1991. In vitro radiation resistance among cell lines established from patients with squamous cell carcinoma of the head and neck. *Cancer* 67, 2741–2747.
- Harari, P.M., Wheeler, D.L., Grandis, J.R., 2009. Molecular target approaches in head and neck cancer: epidermal growth factor receptor and beyond. *Semin. Radiat. Oncol.* 19, 63–68.
- Jiang, N., Wang, D., Hu, Z., Shin, H.J.C., Qian, G., Rahman, M.A., Zhang, H., Amin, A.R.M.R., Nannapaneni, S., Wang, X., et al., 2014. Combination of anti-HER3 antibody MM-121/SAR256212 and cetuximab inhibits tumor growth in preclinical models of head and neck squamous cell carcinoma. *Mol. Canc. Therapeut.* 13, 1826–1836.
- Kazemi, S., Kawaguchi, S., Badr, C.E., Mattos, D.R., Ruiz-Saenz, A., Serrill, J.D., Moasser, M.M., Dolan, B.P., Paavilainen, V.O., Oishi, S., McPhail, K.L., Ishmael, J.E., 2021. Targeting of HER/ErbB family proteins using broad spectrum Sec61 inhibitors coibamide A and apratoxin A. *Biochem. Pharmacol.* 183, 114317.
- Keller, A., Nesvizhskii, A.I., Kolker, E., Aebersold, R., 2002. Empirical statistical model to estimate the accuracy of peptide identifications made by MS/MS and database search. *Anal. Chem.* 74, 5383–5392.
- Khan, T., Kryza, T., Lyons, N.J., He, Y., Hooper, J.D., 2021. The CDCP1 signaling hub: a target for cancer detection and therapeutic intervention. *Canc. Res.* 81, 2259–2269.
- Kunz, V., Bommert, K.S., Kruk, J., Schwinning, D., Chatterjee, M., Stühmer, T., Bargou, R., Bommert, K., 2020. Targeting of the E3 ubiquitin-protein ligase HUWE1 impairs DNA repair capacity and tumor growth in preclinical multiple myeloma models. *Sci. Rep.* 10, 18419.
- Law, M.E., Corsino, P.E., Jahn, S.C., Davis, B.J., Chen, S., Patel, B., Pham, K., Lu, J., Sheppard, B., Norgaard, P., et al., 2013. Glucocorticoids and histone deacetylase inhibitors cooperate to block the invasiveness of basal-like breast cancer cells through novel mechanisms. *Oncogene* 32, 1316–1329.
- Law, M.E., Ferreira, R.B., Davis, B.J., Higgins, P.J., Kim, J.S., Castellano, R.K., Chen, S., Luesch, H., Law, B.K., 2016. CUB domain-containing protein 1 and the epidermal growth factor receptor cooperate to induce cell detachment. *Breast Cancer Res.* 18, 80.
- Liu, Y., Law, B.K., Luesch, H., 2009. Apratoxin A reversibly inhibits the secretory pathway by preventing cotranslational translocation. *Mol. Pharmacol.* 76, 91–104.
- Luesch, H., Chanda, S.K., Raya, R.M., DeJesus, P.D., Orth, A.P., Walker, J.R., Belmonte, J.C.I., Schultz, P.G., 2006. A functional genomics approach to the mode of action of apratoxin A. *Nat. Chem. Biol.* 2, 158–167.
- Luesch, H., Paavilainen, V.O., 2020. Natural products as modulators of eukaryotic protein secretion. *Nat. Prod. Rep.* 37, 717–736.
- Luesch, H., Yoshida, W.Y., Moore, R.E., Paul, V.J., Corbett, T.H., 2001. Total structure determination of apratoxin A, a potent novel cytotoxin from the marine cyanobacterium *Lyngbya majuscula*. *J. Am. Chem. Soc.* 123, 5418–5423.
- Matthew, S., Schupp, P.J., Luesch, H., 2008. Apratoxin E, a cytotoxic peptolide from a Guamanian collection of the marine cyanobacterium *Lyngbya bouillonii*. *J. Nat. Prod.* 71, 1113–1116.
- Nesvizhskii, A.I., Keller, A., Kolker, E., Aebersold, R., 2003. A statistical model for identifying proteins by tandem mass spectrometry. *Anal. Chem.* 75, 4646–4658.
- Paatero, A.O., Kellosalo, J., Dunyak, B.M., Almaliti, J., Gestwicki, J.E., Gerwick, W.H., Taunton, J., Paavilainen, V.O., 2016. Apratoxin kills cells by direct blockade of the Sec61 protein translocation channel. *Cell Chem. Biol.* 23, 561–566.
- Prior, I.A., Lewis, P.D., Mattos, C.A., 2012. Comprehensive survey of RAS mutations in cancer. *Canc. Res.* 72, 2457–2467.
- Qiu, B., Tan, A., Veluchamy, A.B., Li, Y., Murray, H., Cheng, W., Liu, C., Busoy, J.M., Chen, Q.-Y., Sistla, S., et al., 2019. Apratoxin S4 inspired by a marine natural product, a new treatment option for ocular angiogenic diseases. *Investig. Ophthalmol. Vis. Sci.* 60, 3254–3263.
- Ruiz-Saenz, A., Sandhu, M., Carrasco, Y., Maglathlin, R.L., Taunton, J., Moasser, M.M., 2015. Targeting HER3 by interfering with its Sec61-mediated cotranslational insertion into the endoplasmic reticulum. *Oncogene* 34, 5288–5294.
- Singh, S., Ng, J., Sivaraman, J., 2021. Exploring the “other” subfamily of HECT E3-ligases for therapeutic intervention. *Pharmacol. Ther.* 224, 107809.
- Suda, K., Murakami, I., Katayama, T., Tomizawa, K., Osada, H., Sekido, Y., Maehara, Y., Yatabe, Y., Mitsudomi, T., 2010. Reciprocal and complementary role of MET amplification and EGFR T790M mutation in acquired resistance to kinase inhibitors in lung cancer. *Clin. Cancer Res.* 16, 5489–5498.
- Tang, Z., Du, R., Jiang, S., Wu, C., Barkauskas, D.S., Richey, J., Molter, J., Lam, M., Flask, C., Gerson, S., et al., 2008. Dual MET-EGFR combinatorial inhibition against T790M-EGFR-mediated erlotinib-resistant lung cancer. *Br. J. Cancer* 99, 911–922.
- Tranter, D., Paatero, A.O., Kawaguchi, S., Kazemi, S., Serrill, J.D., Kellosalo, J., Vogel, W.K., Richter, U., Mattos, D.R., Wan, X., et al., 2020. Coibamide A targets Sec61 to prevent biogenesis of secretory and membrane proteins. *ACS Chem. Biol.* 15, 2125–2136.
- Uekita, T., Fujii, S., Miyazawa, Y., Iwakawa, R., Narisawa-Saito, M., Nakashima, K., Tsuta, K., Tsuda, H., Kiyono, T., Yokota, J., et al., 2014. Oncogenic Ras/ERK signaling activates CDCP1 to promote tumor invasion and metastasis. *Mol. Cancer Res.* 12, 1449–1459.
- Wu, P., Cai, W., Chen, Q.-Y., Xu, S., Yin, R., Li, Y., Zhang, W., Luesch, H., 2016. Total synthesis and biological evaluation of apratoxin E and its C30 epimer: configurational reassignment of the natural product. *Org. Lett.* 18, 5400–5403.